東海大学紀要海洋学部「海―自然と文化」 第6巻第2号　15-26頁（2008）
Journal of The School of Marine Science and Technology, Tokai University, Vol.6, No.2, pp. 15-26, 2008

初期カルデラ形状をコントロールするファクタ; 数値シミュレーションによる定量的な推定

楠本成寿*1・竹村恵二*2

Control factors on initial caldera geometry; quantitative estimation by numerical simulation

Shigekazu KUSUMOTO and Keiji TAKEMURA

Abstract

In this study we demonstrate that the important factors that control initial caldera geometry are the radius and depth of the magma chamber and the elastic constants of the crust. We approximate the collapse of the magma chamber by the contraction of a small sphere (point source) in an elastic medium, and calculate the surface distribution of the rupture area using the Coulomb failure criterion under the assumption of an elastic-perfectly plastic material. As a result, it was shown that the funnel and piston calderas can be formed by the same collapse mechanism and physical processes, and the geometry of the caldera is controlled by the depth and radius of the magma chamber and the proportionality coefficient in the linear relationship between the caldera radius and the magma chamber depth. In the case that values of Poisson's ratio, Young's modulus, compressive strength and angle of internal friction are given in the wide range covering almost all igneous rocks, it was found that the coefficient is strongly dependent on the Poisson's ratio. In addition, it was found that the volume change required for the caldera formation is described by a third-power polynomial expression of the depth of the magma chamber. Although the physical meaning of each coefficient is unknown at present, it was shown that the third degree of the polynomial is the most important term.

Keywords: caldera, caldera geometry, depth of magma chamber, Poisson's ratio, numerical simulation

1. Introduction

Calderas are kilometre-scale volcanic depressions by partial or total collapse of a magma chamber roof (e.g., Smith and Bailey, 1968; Druitt and Sparks, 1984; Lipman, 1997). Although the process of caldera collapse depends on many factors, it is known that the key element in caldera formation is the removal of magmatic support from the magma chamber, as a classic formation mechanics (e.g., Anderson, 1936; Williams, 1941; Druitt and Sparks, 1984; Scandone, 1990; Lipman, 1997). In addition, properties of the host rock such as topographic load, pre-existing structures and rheological properties play an important role for caldera formation. (e.g., Folch and Marti, 2004; Pinel and Jaupart, 2005; Trasatti *et al*., 2005).

The structures of calderas have been investigated by both field studies and analogue models (e.g., Yoshida, 1984; Komuro, 1987; Kamata, 1989; Marti *et al*., 1994; Lipman, 1997; Acocella *et al*., 2000, 2004; Roche et al., 2000; Walter and Troll, 2001; Troll *et al*., 2002; Holohan *et al*., 2005). Recent laboratory experiments and field studies have shown that piston- and funnel-type calderas have the same collapse mechanism and general physical processes. Namely, it was suggested that the size and

2008年6月9日受理
＊1　東海大学海洋学部（School of Marine Science and Technology, Tokai University）
＊2　京都大学大学院理学研究科附属地球熱学研究施設（Beppu Geothermal Research Laboratory, Kyoto University）

depth of the magma chamber are important factors governing the type of caldera (e.g., Roche *et al*., 2000; Lipman, 1997).

On the other hand, numerical simulations have been used to provide quantitative estimates of the distribution of the ring fault system associated with calderas (Gudmundsson *et al*., 1997; Gudmundsson, 1998a; Kusumoto and Takemura, 2003; Folch and Marti, 2004). Numerical and analogue modellings have demonstrated that both the geometry of the magma chamber and the loading conditions play an important role in determining caldera geometry and structure (e.g., Gudmundsson *et al*., 1997; Gudmundsson, 1998a; Kusumoto and Takemura, 2003; Acocella *et al*., 2004; Holohan *et al*., 2005). Kusumoto and Takemura (2005) showed that the necessary contraction for the caldera formation is described by fifth-power polynomial expression of the depth of the magma chamber. However, it is difficult that the contraction of the magma chamber is the optimum index for understanding caldera formation, as compared with volume change. Thus, in this study, we attempted to clarify the relationship between the depth and volume change of the magma chamber and to estimate the factors that control initial caldera geometry.

For the purpose of analysing and making the model mathematically tractable, in our simulations, collapse of the magma chamber is approximated by the volume decrease of a small sphere (point source: Mogi model (Mogi, 1958)) in an elastic medium, while the distribution of surface rupturing is calculated using the Coulomb failure criterion under the assumption of an elastic-perfectly plastic material (Fig. 1). The elastic-plastic boundary is assumed to be the location of the ring fault that constructs the initial caldera.

The limitations of the point source model are well known (e.g., McTigue, 1987; Gudmundsson, 1998a, 1998b;

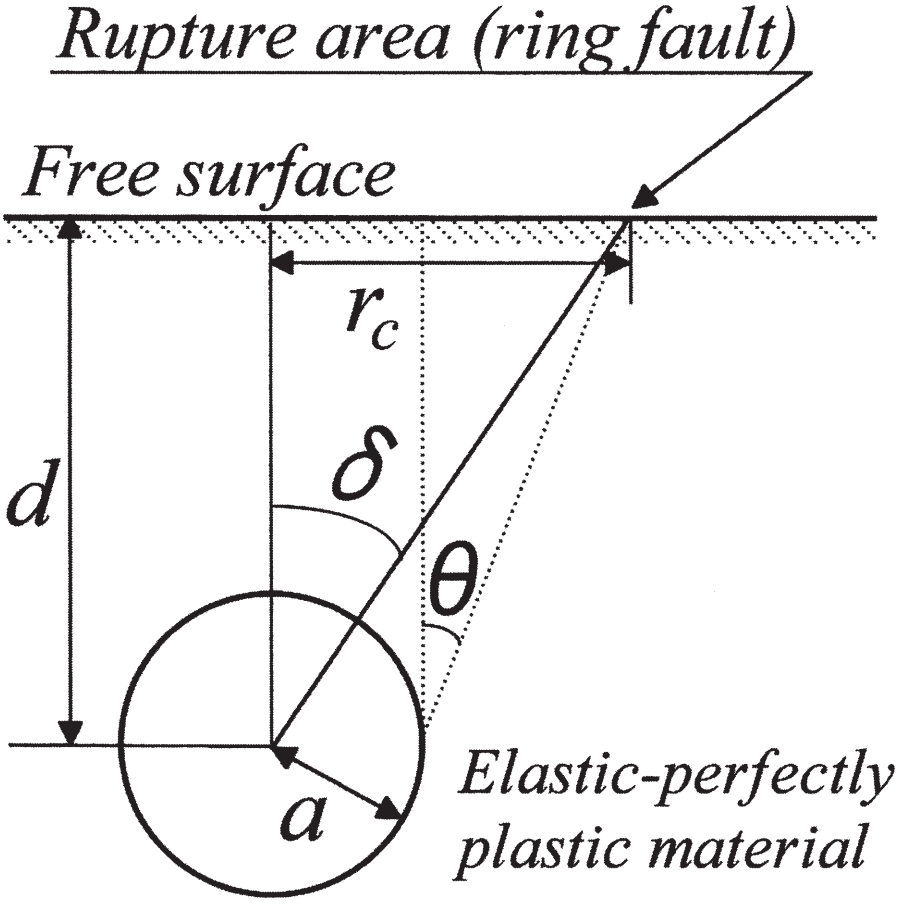

Fig. 1 Model of spherical magma chamber of radius a and depth to centre d, where r_c is the horizontal distance from surface point located at the top of the magma chamber to the rupture area (ring fault). The crust is assumed to be an elastic-perfectly plastic material. δ: angle between the centre of the magma chamber and the initial caldera boundary. θ: angle between the initial caldera boundary and the perpendicular line drawn from the edge of the chamber to the surface.

Trasatti *et al*., 2005). For example, the differences between solutions derived from the point source model and finite sphere model for a vertical deformation are significant, and are much greater than the accuracy of modern geodetic surveys. However, in this study we use a point source model that facilitates mathematical treatment rather than the finite sphere model and an ellipsoidal model that is widely regarded as the typical shape of a magma chamber. This choice is valid for the purpose of our study, as the difference between the point source model and finite sphere model solutions in terms of the surface pattern of rupture area is minor and does not negatively influence our investigation (e.g. Kusumoto and Takemura, 2005).

2. Model and Simulations

Considering the relationship between the internal pressure change (Δp) of a sphere and volume change (ΔV), $\Delta p=\mu\Delta V/\pi a^3$, the surface strain fields due to radial deformation of a small sphere provided by Kusumoto and Takemura (2005) are obtained as follows:

$$\varepsilon_{xx}=\frac{\Delta V}{2\pi R^3}\frac{\lambda+2\mu}{\lambda+\mu}\left(1-\frac{3x^2}{R^2}\right),\quad \varepsilon_{yy}=\frac{\Delta V}{2\pi R^3}\frac{\lambda+2\mu}{\lambda+\mu}\left(1-\frac{3y^2}{R^2}\right),$$
$$\varepsilon_{zz}=-\frac{\Delta V}{2\pi R^3}\frac{\lambda}{\lambda+\mu}\left(1-\frac{3d^2}{R^2}\right),\quad \varepsilon_{xy}=-\frac{3\Delta V}{2\pi R^3}\frac{\lambda+2\mu}{\lambda+\mu}\frac{xy}{R^2},$$
$$\varepsilon_{yz}=-\frac{3\Delta V}{2\pi R^3}\frac{\lambda+2\mu}{\lambda+\mu}\frac{yd}{R^2},\quad \varepsilon_{zx}=-\frac{3\Delta V}{2\pi R^3}\frac{\lambda+2\mu}{\lambda+\mu}\frac{xd}{R^2}$$

where d, λ and μ are depth of magma chamber and Lame's constants, respectively, and $R^2=x^2+y^2+d^2$. In this study, compression is positive and the decrease of the internal pressure and volume of the small sphere is positive, because phenomena due to the contraction of the magma chamber are discussed. It is known that the Lame's constants have the following relationship with Young's modulus (E) and Poisson's ratio (ν) (e.g., Jaeger *et al*., 2007):

$$E=\frac{\mu(3\lambda+2\mu)}{\lambda+\mu},\quad \nu=\frac{\lambda}{2(\lambda+\mu)}$$

From these equations, we obtain the surface strain fields due to volume change of the magma chamber.

The strain field produced by contraction of the sphere can be transformed into a stress field via Hooke's law. The stress field can then be evaluated using a dimensionless factor F based on the Coulomb failure criterion (e.g., Segall and Pollard, 1980; Jaeger *et al*., 2007), as follows:

$$F\equiv\frac{1}{c_0}\left[\sigma_1-\sigma_3\tan^2\left(45^\circ+\frac{\varphi}{2}\right)\right]$$

where σ_1 and σ_3 are the maximum and minimum principal stresses, respectively, and c_o and φ are the compressive strength and angle of internal friction, respectively. As the crust is assumed to react as an elastic-perfectly plastic material, the area of $F\geq1$ corresponds to the rupture area.

Simulations were conducted assuming basaltic crust with the following elastic constants: Poisson's ratio of 0.25 ($\lambda=\mu$), Young's modulus of 40 GPa, and compression strength (c_o) of 160 MPa (e.g., Lama and Vutukuri, 1978; Gudmundsson, 1988; Yamaji, 2000). The angle of internal friction was assumed to be 30°, consistent with the observed angle for rock near the surface (e.g., Lama and Vutukuri, 1978; Yamaji, 2000).

3. Volume change required for caldera formation

Fig. 2 shows the relationship between depth and volume change of the magma chamber at the first formation of surface rupture area (ring fault). The regression curve that explain the ΔV-d relationship was obtained by a least-squares fit of the data. The ΔV-d relationship is given by

$$\Delta V=\sum_{n=0}^{3}\kappa_n d^n \qquad (1)$$

where $\kappa_0=5.63\times10^{-3}$, $\kappa_1=-9.27\times10^{-5}$, $\kappa_2=1.79\times10^{-4}$ and $\kappa_3=9.30\times10^{-3}$. The volume change required for the ring fault initiation is described by a third-power polynomial expression of the depth of the magma chamber, and is 0.04, 0.07, 0.26 and 1.18km^3 in each case of $d=1.5$, 2.0, 3.0 and 5.0km. As we selected the lowest degree consistent with the data, the physical meaning of each coefficient is currently unknown. However, we expect that equation (1) is free of serious error, as the volume change required for caldera formation is described by a polynomial of d and the dimension of the highest degree of the right hand of the equation (1) is equal to the dimension of the left hand. In addition, the magnitude of the coefficient of the highest degree is an order of magnitude larger than the other coefficients. Thus, the third degree of the equation is the most important term.

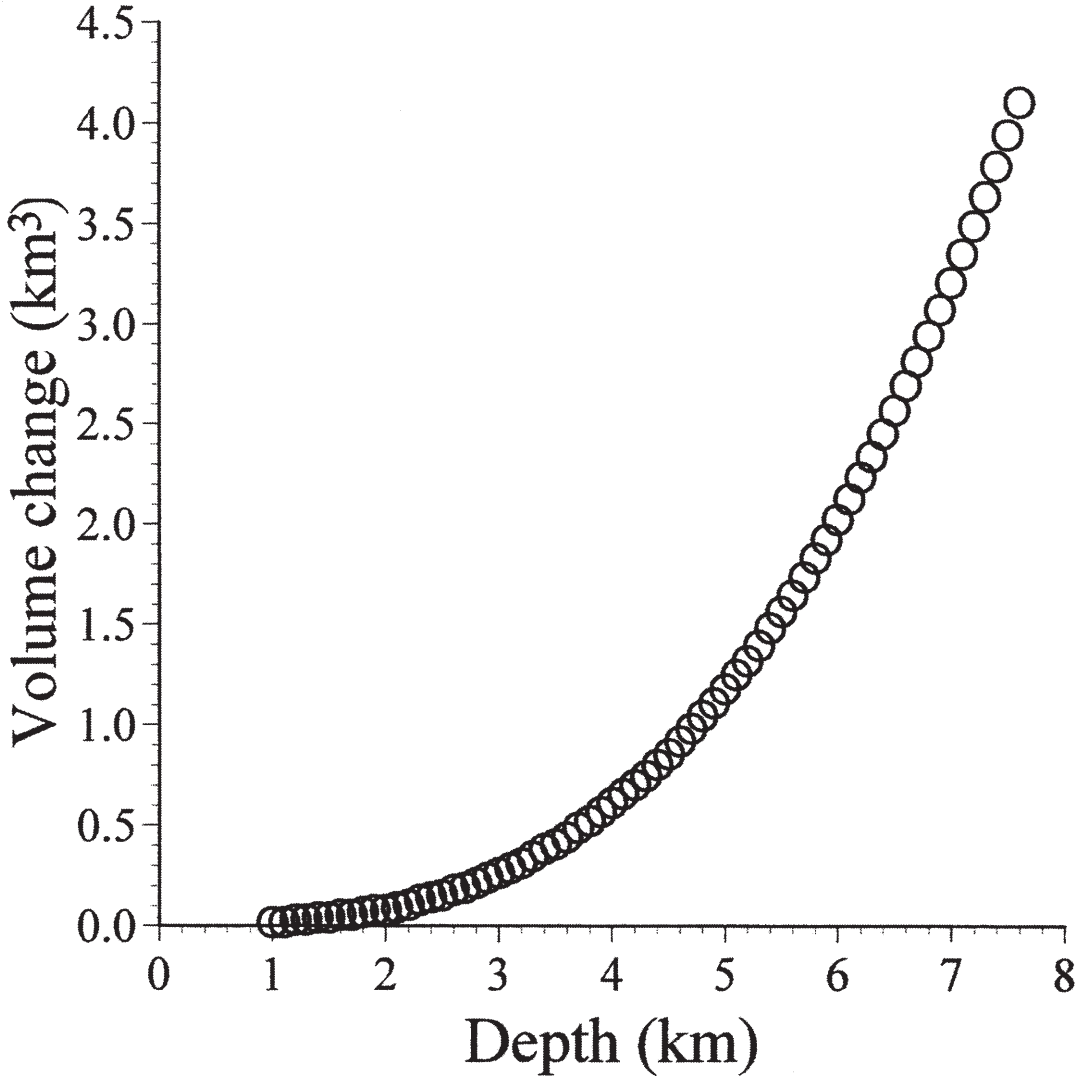

Fig. 2 The ΔV-d relationship between depth and contraction of the magma chamber. The volume change required for the initiation of caldera formation is described by a polynomial of d.

4. Caldera radius and depth of magma chamber

Fig. 3 shows the relationship between depth and the horizontal distance (r_c) from a surface point located at the top of the magma chamber to the ring fault. There are small dispersions in the data shown in Fig. 3. Although these dispersions are caused by the numerical instability due to rough spacing of the calculation point, the dispersions do not give serious errors in the estimation of the proportionality coefficient. The r_c-d relation is given by

$$r_c = \alpha d \qquad (2)$$

where $\alpha = 0.82$. The proportionality coefficient, α, indicates that the angle between the centre of the magma chamber and the initial caldera boundary (δ; Fig. 1) is always approximately 39.4°. We expect that the linear relationship probably stems from the assumption of the elastic-perfectly plastic material that stress is proportional to strain below the yield stress. It would be free of serious error to approximate the behaviour of the crust as an elastic-perfectly plastic material, as caldera collapse would occur readily.

In terms of dimension analyses, the proportionality coefficient α would be a dimensionless constant.

5. Proportionality coefficient α

Although the relationship shown as equation (2) has been already given by Kusumoto and Takemura (2005), the detailed discussions on this proportionality coefficient, α, have not been carried out yet. Here, we attempted to

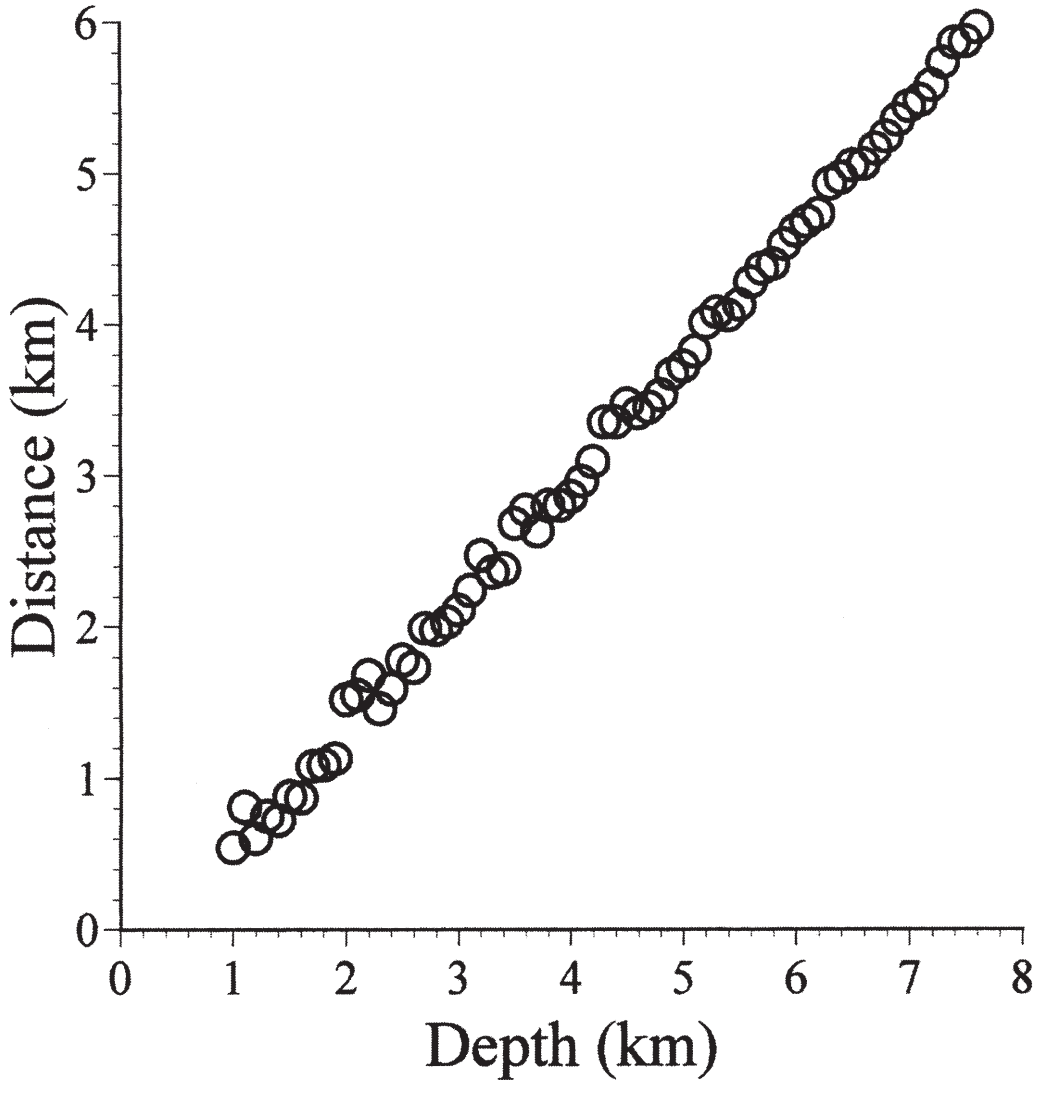

Fig. 3 The r_c-d relationship between depth and horizontal distance from the top of the magma chamber to the rupture area. The radius of the initial caldera is dependent upon the depth of the magma chamber.

discuss characteristics of the coefficient α.

We can expect that the proportionality coefficient α is controlled by the compressive strength, angle of internal friction, Poisson's ratio and Young's modulus, as the coefficient is obtained via the Coulomb failure criterion. As the compressive strength and Young's modulus are directly related to the development of surface ruptures, we first calculated the sensitivity of α to variations in these factors.

Calculations were performed following Calculation I in Table 1. Namely, although the angle of internal friction and Poisson's ratio are constants of 30° and 0.25, respectively, the compressive strength and Young's modulus are varied from 5 to 500 MPa (e.g., Lama and Vutukuri, 1978; Yamaji, 2000) and from 10 to 100 GPa (e.g., Lama and Vutukuri, 1978; Turcotte and Schubert, 1982), respectively. Fig. 4 shows the result of the calculation I. For a small compressive strength, α is strongly dependent on the magnitude of the Young's modulus, however, for compressive strength of >35 MPa, there is no characteristic distribution on α. Fig. 5 provides a histogram of α. The frequency count of α has a peak between 0.82 and 0.83, with the minimum, average and maximum values of α being 0.78, 0.82 and 0.84, respectively. The difference between maximum and minimum values is 0.06.

To clarify whether the Poisson's ratio and angle of internal friction influence the magnitude of α, the distributions of the coefficient α were estimated by following Calculations II and III in Table 1. The ranges of values of the Poisson's ratio and angle of internal friction are based on observed data shown in Lama and Vutukuri

Table 1: Conditions of compressive strength, angle of internal friction, Poisson's ratio and Young's modulus for various calculations of the coefficient α. The ranges of values of these constants are based on observed data shown in Lama and Vutukuri (1978), Turcotte and Schubert (1982) and Yamaji (2000), and cover almost all igneous rocks.

	Calculation I	Calculation II	Calculation III	Calculation IV
Poisson's ratio (ν)	0.25	0.05 → 0.45	0.25	0.05 → 0.45
Angle of internal friction (φ)	30°	30°	5° → 45°	5° → 45°
Compressive strength (c_o)	5 MPa → 500 MPa	5 MPa → 500 MPa	5 MPa → 500 MPa	5 MPa → 500 MPa
Young's modulus (E)	10 GPa → 100 GPa	10 GPa → 100 GPa	10 GPa → 100 GPa	10 GPa → 100 GPa

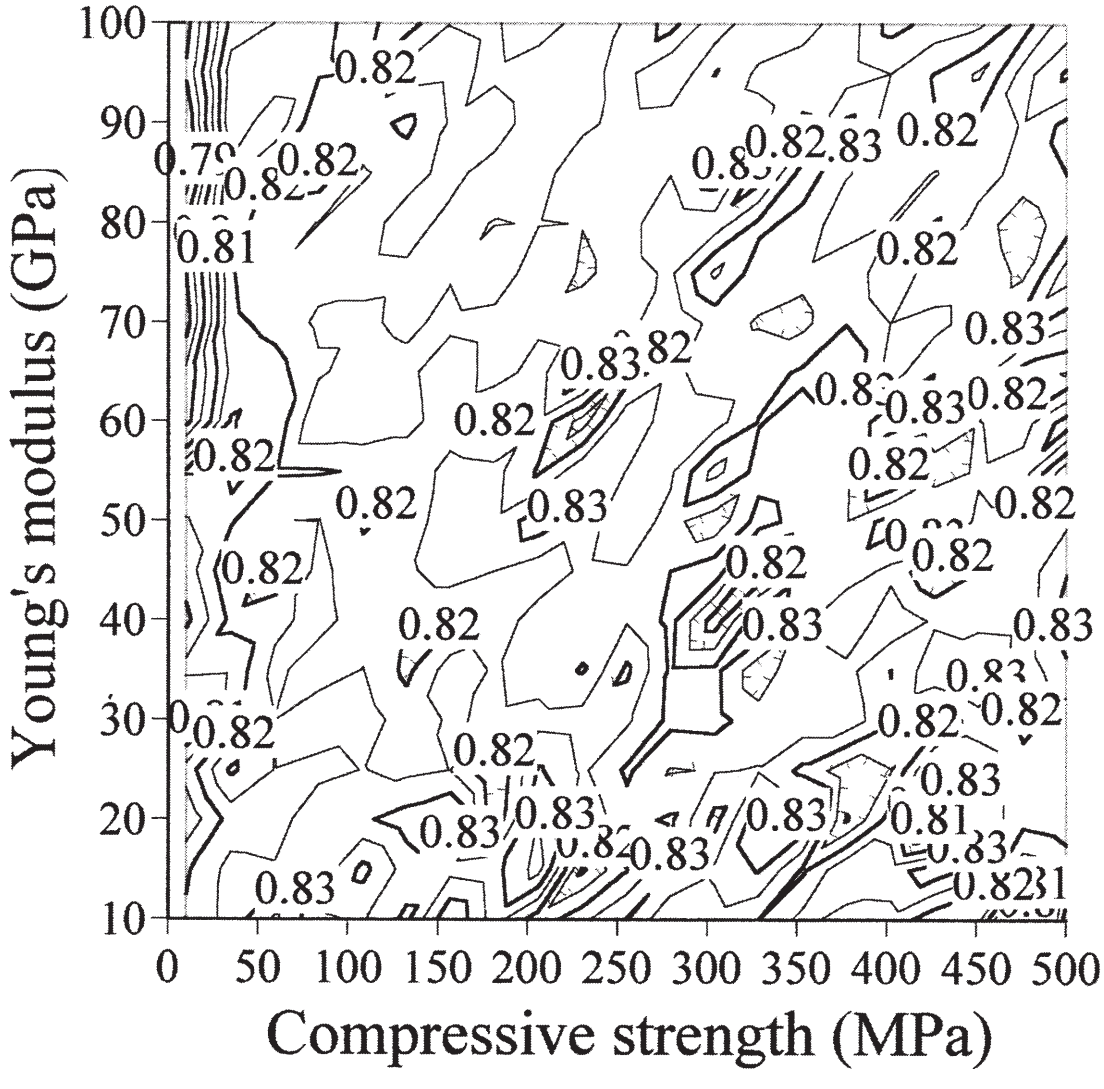

Fig. 4 Distribution of the coefficient α, which determines the radius of the initial caldera. The compressive strength and Young's modulus are varied from 5 to 500 MPa and from 10 to 100 GPa respectively. In this calculation, the angle of internal friction and Poisson's ratio are constants of 30° and 0.25, respectively. (c.f., Calculation I in Table 1)

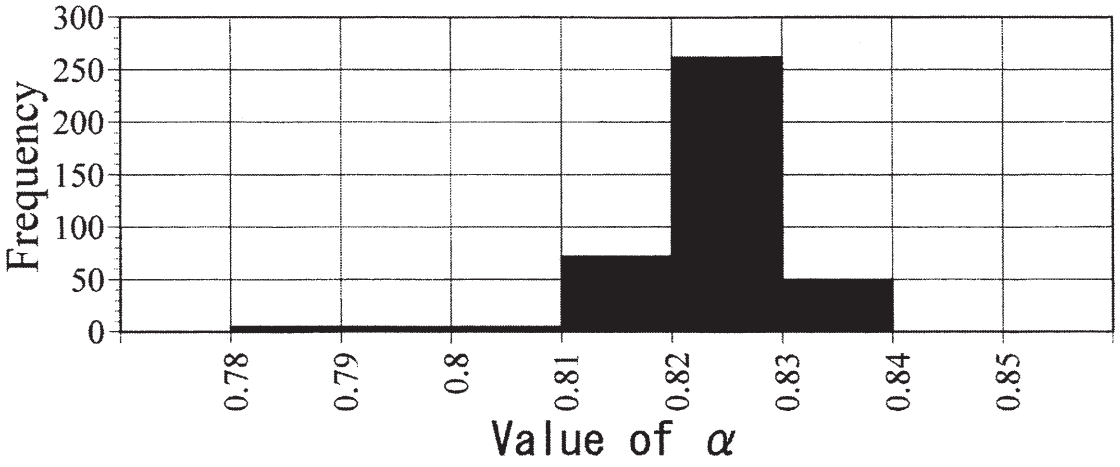

Fig. 5　Histogram of α values shown in Figure 4.

(1978) and Turcotte and Schubert (1982) and cover almost all igneous rocks.

The results are shown in Figs. 6 and 7 and Tables 2 and 3. The difference between maximum and minimum values by change of Poisson's ratio is 1.11 (Table 2). And the same difference by change of the angle of internal friction is 0.39 (Table 3). These results indicate that changes in the Poisson's ratio and angle of internal friction have a greater effect on α than the effect of changes in the compressive strength and Young's modulus on α.

Fig. 8 shows the distribution of α derived from Calculation IV in Table 1. In this calculation, we evaluated effects that combination of the Poisson's ratio and angle of internal friction gives magnitude of α. The compressive strength and Young's modulus were changed in all combinations of the mentioned two elastic constants (Table 1). The magnitudes of α shown in this figure are averages of the values given by calculations in each combination of Poisson's ratio-angle of internal friction. In case of the combination of $\phi=30^\circ$ and $\nu=0.25$, α in Fig. 8 is 0.82 and is the same as the average value given in Calculation I. The α distribute between 0.53 and 1.72.

From Figs. 6, 7 and 8, we can find that the magni tude of α is especially sensitive to changes in the Poisson's ratio.

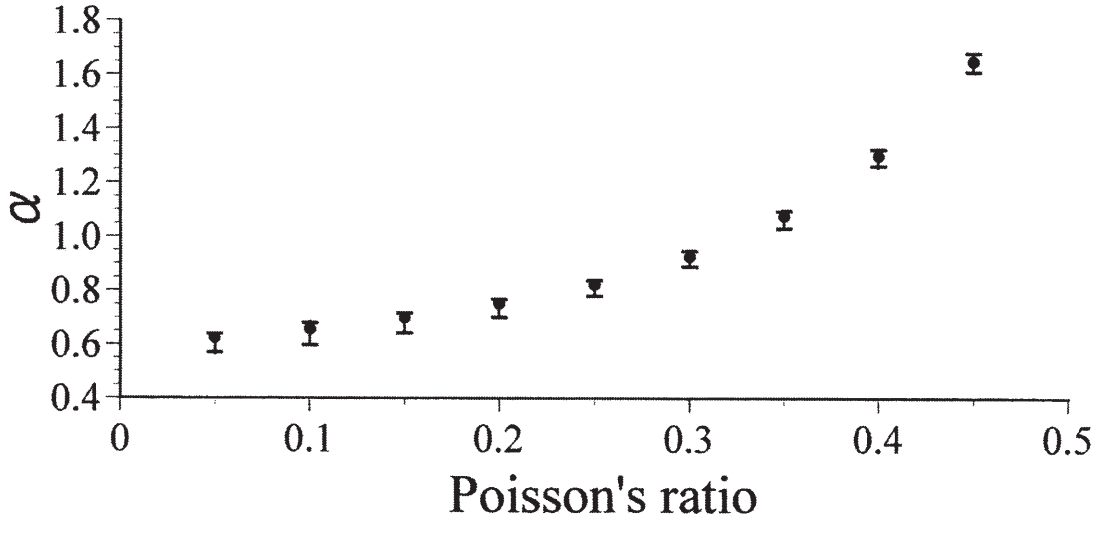

Fig. 6　Changes in α with varying Poisson's ratio. The detailed values are given in Table 2. The calculations are as described by Calculation II in Table 1.

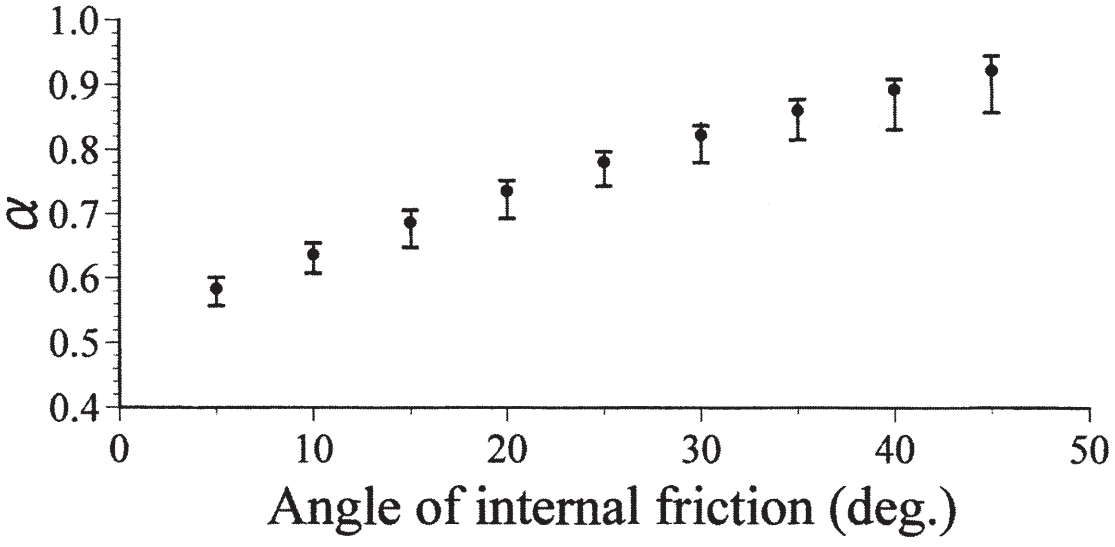

Fig. 7 Variations in α with changes in the angle of internal friction. The detailed values are given in Table 3. The calculations are as described by Calculation III in Table 1. The effect on α of changes in the angle of internal friction is greater than the effect on α of changes in compressive strength and Young's modulus.

Table 2: Table of α by change of Poisson's ratio. The difference between maximum and minimum values is 1.11. And the same difference on averaged values of α is 1.03. Change of Poisson's ratio influences magnitude of α and radius and geometry of the caldera.

Poisson's ratio (ν)	minimum	average	maximum
0.05	0.57	0.62	0.64
0.10	0.60	0.65	0.68
0.15	0.64	0.70	0.72
0.20	0.70	0.75	0.77
0.25	0.78	0.82	0.84
0.30	0.90	0.93	0.95
0.35	1.03	1.08	1.10
0.40	1.26	1.30	1.32
0.45	1.61	1.65	1.68

Table 3: Table of α by change of angle of internal friction. The difference between maximum and minimum values is 0.39. And the same difference on averaged values of α is 0.34. Change of angle of internal friction as well as Poisson's ratio influences magnitude of α and radius and geometry of the caldera.

Angle of internal friction (φ: deg.)	minimum	average	maximum
5	0.56	0.58	0.60
10	0.61	0.64	0.65
15	0.65	0.69	0.71
20	0.69	0.74	0.75
25	0.74	0.78	0.80
30	0.78	0.82	0.84
35	0.82	0.86	0.88
40	0.83	0.89	0.91
45	0.86	0.92	0.95

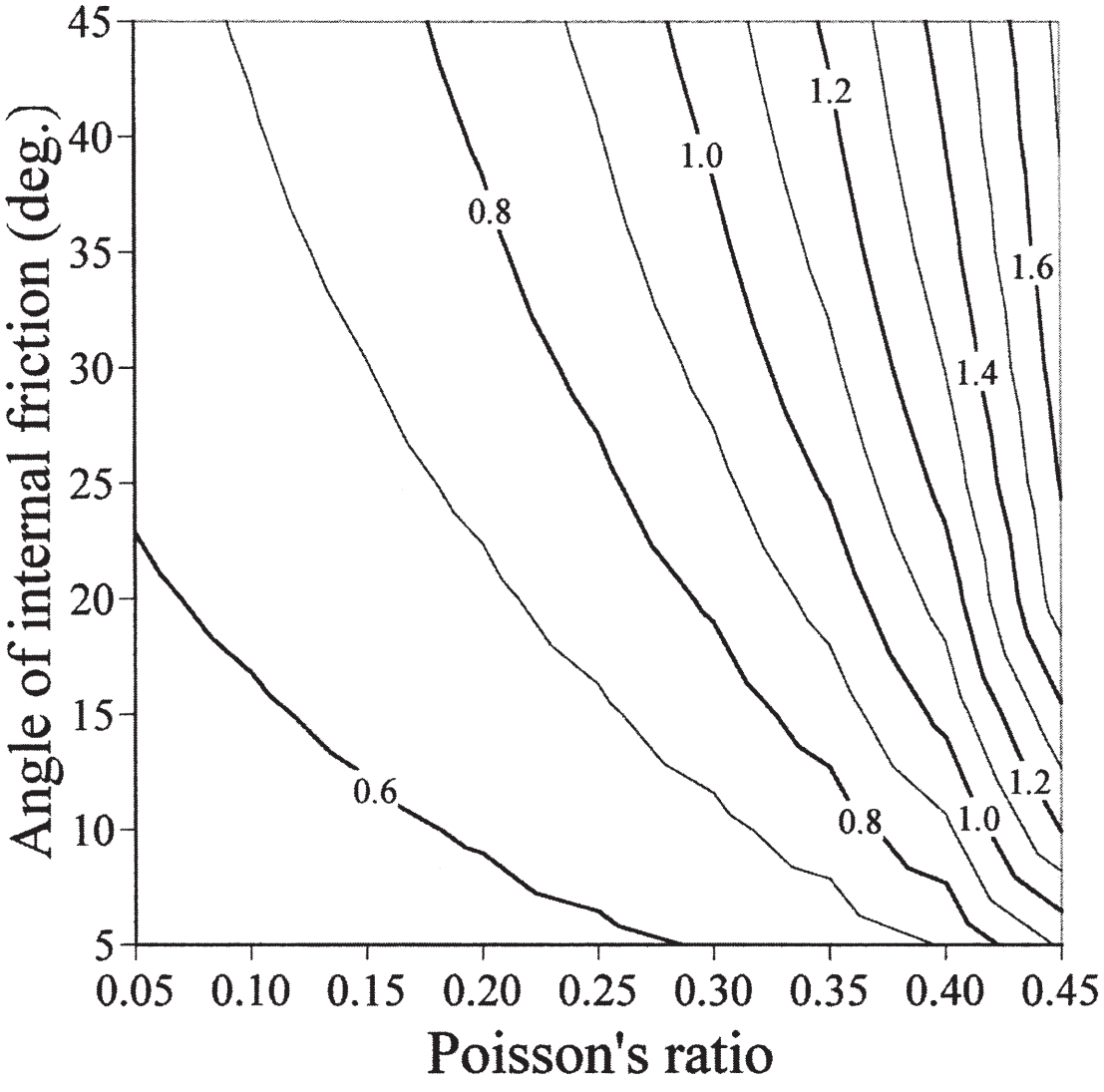

Fig. 8　Distribution of the coefficient α given by calculation IV in Table 1. All of the elastic constants are independently changed and all their combinations are considered. Here, α are averages of calculated values.

6. Control factor on caldera geometry and type

Fig. 9 shows the relationship between the depth of the magma chamber and the angle between the initial caldera boundary at the surface and a perpendicular line drawn from the edge of the chamber to the surface (θ; Fig. 1). In the calculation, we employed $E=40$ GPa, $\nu=0.25$, $\varphi=30^\circ$ and $c_o=160$ MPa. Because the caldera geometry can be estimated from magnitude of θ as shown in Fig. 1, the θ is the parameter that indicates the radius, geometry and type of the caldera.

A negative angle ($\theta\leq 0$) indicates that the radius of the initial caldera is smaller than the radius of the magma chamber. This would produce a piston caldera with outward-dipping or vertical ring faults (e.g., Yoshida, 1984; Rymer *et al*., 1998; Roche *et al*., 2000). By Roche *et al*. (2000), it is shown that the reverse fault with dip angle of 50° - 80° is formed before the formation of the normal fault, in roof aspect ratio of 0.2. This aspect ratio of 0.2 is equivalent to $d/a=1.4$ in this study. In this case, the formation of the reverse fault with the dip angle 80° ($\theta=-10$ in Fig. 9) is expected and this is consistent with the analogue experiments (Roche *et al*., 2000).

In contrast, a result of $\theta > 0$ indicates that the radius of the initial caldera is larger than the radius of the chamber. This would produce a funnel caldera or piston caldera with inward-dipping ring fault (e.g., Lipman, 1984; Kamata, 1989; Roche *et al*., 2000). Despite potential differences in the medium and model assumed

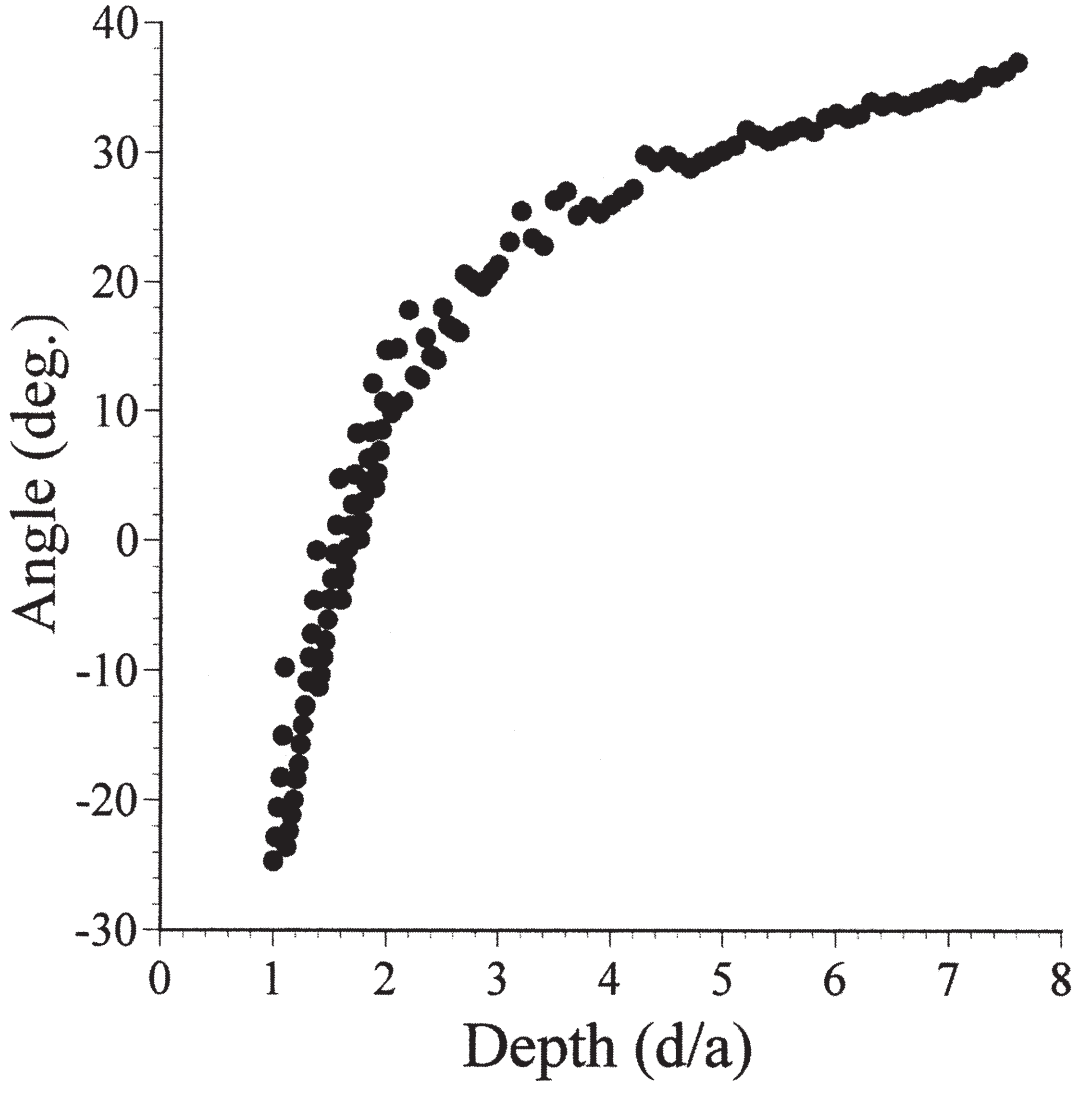

Fig. 9 Relationship between depth of the magma chamber and the angle θ. The sign and magnitude of θ indicate caldera type: $\theta \leq 0$ indicates the formation of a piston caldera with outward-dipping or vertical ring faults, while $\theta > 0$ indicates the formation of a piston or funnel caldera with inward -dipping ring faults.

in this study, our results (Fig. 9) are consistent with the findings of Roche *et al*. (2000) and Lipman (1997). Namely, funnel and piston calderas have the same collapse mechanism and physical processes, and the geometry of the caldera is controlled by the depth of the magma chamber.

The value of the parameter θ is dependent on the depth of the magma chamber, as shown in Fig. 9. In contrast, θ is the parameter that is determined geometrically, as shown in Fig. 1, and is described as follows:

$$\theta = \frac{180^\circ}{\pi} \tan^{-1}\left(\frac{r_c - a}{d}\right) \qquad (3)$$

Considering equation (2), the following equation is derived.

$$\theta = \frac{180^\circ}{\pi} \tan^{-1}\left(\alpha - \frac{a}{d}\right) \qquad (4)$$

Equation (4) has a negative value at $\alpha \leq a/d$ and a positive value at $\alpha > a/d$ and indicate that the caldera geometry can be determined by combination of α, a and d. As shown in previous section, the coefficient α is dependent on Poisson's ratio strongly. Hence, we can suggest that the caldera geometry including type of caldera is controlled by the radius and depth of the magma chamber and the Poisson's ratio of the crust.

In our simulations, we employed a point source model embedded in a homogeneous elastic medium, and formation of the caldera was examined by evaluating the surface stress field due to contraction of the point source. Thus, our solutions do not have enough accuracy

to discuss detailed caldera formation by applying the results to field data. However, our findings concerning the volume change required for caldera formation and our conclusion that Poisson's ratio of the medium and the depth and radius of the magma chamber will play an important role in determining caldera geometry provide useful first-order information for future practical simulations. For example, the depth of the magma chamber will be estimated by applying the caldera radius observed in the field to the equation (2) and the volume required for caldera formation can be evaluated by applying the depth to the equation (1).

7. Conclusions

In order to estimate the factors controlling the initial caldera geometry, we used numerical simulations based on the point source model assumed in the homogeneous elastic medium. In this study, we approximated the collapse of the magma chamber by the contraction of the source and calculated the surface distribution of the ring fault using the Coulomb failure criterion under the assumption of an elastic-perfectly plastic material.

As a result, it was shown that the funnel and piston calderas can be formed by the same collapse mechanism and physical processes, and the geometry of the caldera is controlled by the depth and radius of the magma chamber and the proportionality coefficient in the linear relationship between the caldera radius and magma chamber depth. This proportionality coefficient is strongly dependent on the Poison's ratio basically. In the case of shallow magma chamber, the dip angle of ring fault given by our result was consistent with the analogue experiments.

In addition, it was found that the volume change required for the initiation of caldera formation is described by a third-power polynomial expression of the depth of the magma chamber. Although the physical meaning of each coefficient is unknown at present, it was shown that the third degree of the polynomial is the most important term. Because the depth of the magma chamber can be estimated by the caldera radius, we expect that this result can evaluate the volume required for caldera formation.

Acknowledgments

This work was done as a part of the Unzen Scientific Drilling Project of the Ministry of Education, Cultures, Sports, Science and Technology of Japan and was also supported by a Grant in Aid for Scientific Research from the Ministry of Education, Cultures, Sports, Science and Technology of Japan (No. 17740292), Tokai University General Research Organization Research Promotion Plan and Overseas research visit program of Tokai University. We are grate thankful to Professor A. Gudmundsson of University of London and Dr. O. Roche for their careful reviews and helpful comments on our manuscript (early version). We are thankful to anonymous reviewer for his or her careful review of the paper and helpful comments on the manuscript.

References

Acocella, V., F. Cifelli and R. Funiciello (2000): Analogue models of collapse calderas and resurgent domes. J. Volcanol. Geotherm. Res., **104**, 81-96.

Acocella, V., R. Funiciello, E. Marotta, G. Orsi and S. de Vita (2004): The role of extensional structures on experimental calderas and resurgence. J. Volcanol. Geotherm. Res., 129, 199-217.

Anderson, E. M. (1936): The dynamics of formation of cone sheets, ring dykes and cauldron subsidences. Proc. R. Soc. Edinb., **56**, 128-163.

Druitt, T. H. and R. S. Sparks (1984): On the formation of calderas during ignimbrite eruptions. Nature, **310**, 679-681.

Folch, A. and J. Marti (2004): Geometrical and mechanical constraints on the formation of ring-fault calderas. Earth Planet. Sci. Lett., **221**, 215-225.

Gudmundsson, A. (1988): Effect of tensile stress concentration around magma chambers on intrusion and extrusion frequencies. J. Volcanol. Geotherm. Res., **35**, 179-194.

Gudmundsson, A. (1998a): Formation and development of normal-fault calderas and the initiation of large explosive eruptions. Bull. Volcanol., **60**, 160-170.

Gudmundsson, A. (1998b): Magma chambers modeled as cavities explain the formation of rift zone central volcanoes and their eruption and intrusion statistics. J. Geophys. Res., **103**, 7401-7412.

Gudmundsson, A., J. Marti and E. Turon (1997): Stress fields generating ring faults in volcanoes. Geophys. Res. Lett., **24**, 1559-1562.

Holohan, E. P., V. R. Troll, T. R. Walter, S. Munn, S. McDonnell and Z. K. Shipton (2005): Elliptical calderas in active tectonic settings: an experimental approach. J. Volcanol. Geotherm. Res., **144**, 119-136.

Jaeger, J. C., N. G. Cook and R. W. Zimmerman (2007): Fundamentals of Rock Mechanics, 4th edition, Blackwell, Oxford, 475pp.

Kamata, H. (1989): Shishimuta caldera, the buried source of the Yabakei pyroclastic flow in the Hohi volcanic zone, Japan. Bull. Volcanol., **51**, 41–50.

Komuro, H. (1987): Experiments on cauldron formation: a polygonal cauldron and ring fractures. J. Volcanol. Geotherm. Res., **31**, 139–149.

Kusumoto, S. and K. Takemura (2003): Numerical simulation of caldera formation due to collapse of a magma chamber. Geophys. Res. Lett., **30**(24), 2278, doi10.1029/2003GL018380.

Kusumoto, S. and K. Takemura (2005): Caldera geometry determined by the depth of the magma chamber. Earth Planets Space, **57**, e17–e20.

Lama, R. D. and V. S. Vutukuri (1978): Handbook on mechanical properties of rocks–testing techniques and results–vol. 2, Trans Tech Publications, Clausthal, 481pp.

Lipman, P. W. (1984): The roots of ash flow calderas in the western North America: windows into the tops of granitic batholiths. J. Geophys. Res., **89**, 8801–8841.

Lipman, P. W. (1997): Subsidence of ash–flow calderas: relation to caldera size and magma–chamber geometry. Bull. Volcanol., **59**, 198–218.

Marti, J., G. J. Ablay, L. T. Redshaw and R. S. J. Sparks (1994): Experimental studies of collapse calderas. J. Geol. Soc. London, **151**, 919–929.

McTigue, D. F. (1987): Elastic stress and deformation near a finite spherical magma body: resolution of the point source paradox. J. Geophys. Res., **92**, 12931–12940.

Mogi, K. (1958): Relations between the eruptions of various volcanoes and the deformation of the ground surfaces around them. Bull. Earthquake Res. Inst., **36**, 99–134.

Pinel, V. and C. Jaupart (2005): Caldera formation by magma widthdrawal from a reservoir beneath a volcanic edifice. Earth Planet. Sci. Lett., **230**, 273–287.

Roche, O., T. H. Druitt and O. Merle (2000): Experimental study of caldera formation. J. Geophys. Res., **105**, 395–416.

Rymer, H., B. van Vries, J. Stix, J. and G. Williams–Jones (1998): Pit crater structure and processes governing persistent activity at Masaya volcano, Nicaragua. Bull. Volcanol., **59**, 345–355.

Scandone, R. (1990): Chaotic collapse of calderas. J. Volcanol. Geotherm. Res., **42**, 285–302.

Segall. P., and D. D. Pollard (1980): Mechanics of discontinuous faults. J. Geophys. Res., **85**, 4337–4350.

Smith, R. L. and R. A. Bailey (1968): Resurgent cauldrons. Geol. Soc. Am. Mem., **116**, 613–662.

Trasatti, E., C. Giunchi and M. Bonafede (2005): Structural and rheological constants on source depth and overpressure estimates at the Campi Flegrei caldera, Italy. J. Volcanol. Geotherm. Res., **144**, 105–118.

Troll, V. R., T. R. Walter and H. –U. Schmincke (2002): Cyclic caldera collapse: Piston or piecemeal subsidence? Field and experimental evidence. Geology, **30**, 135–138.

Turcotte, D. L. and G. Schubert (1982): Geodynamics: applications of continuum physics to geological problems. John Wiley & Sons, New York, 450pp.

Walter, T. R. and V. R. Troll (2001): Formation of caldera periphery faults: An experimental study. Bull. Volcanol., **63**, 191–203.

Williams, H. (1941): Calderas and their origin. Bull. Dep. Geol. Sci., 25. Univ. Californ. Publ., 239–346.

Yamaji, A. (2000): [Introduction to theoretical tectonics], Asakura Syoten, Tokyo, 287pp. (in Japanese).

Yoshida, T. (1984): Tertiary Ishizuki cauldron, southwestern Japan arc formation by ring fracture subsidence. J. Geophys. Res., **89**, 8502–8510.

要　旨

初期カルデラ形状をコントロールする重要なファクタは，マグマ溜りの半径と深さ，そして地殻の弾性定数であることを，本研究で明らかにした．マグマ溜りの崩壊を弾性体中の小球の収縮で近似し，弾完全塑性体の仮定の下，クーロン破壊基準を用いて地表面の破壊領域の分布を計算した．その結果，じょうご型カルデラとピストン型カルデラは，同じ崩壊メカニズムと物理プロセスにより形成されることが明らかになった．また，カルデラの形状は，マグマ溜りの半径と深さ，そしてカルデラ半径とマグマ溜り深さの間の線形関係を説明する比例係数によりコントロールされることが明らかにされた．ポアソン比，ヤング率，圧縮強度，内部摩擦角がほとんど全ての火成岩をカバーするような広い範囲で与えられた場合，その比例係数は，ポアソン比に強く依存していることが明らかにされた．また，カルデラ形成に必要とされる体積変化量は，マグマ溜りの深さの 3 次式によって記述されることが明らかにされた．各係数の物理的な意味は現段階では不明であるが，多項式の 3 次の項が最も重要な項であることが示された．

キーワード：カルデラ，カルデラ形状，マグマ溜りの深さ，ポアソン比，数値シミュレーション